Electronic Supplementary Material (ESI) for Sustainable Energy & Fuels.

Enhancing bio-oil quality and energy recovery by atmospheric hydrodeoxygenation of wheat straw pyrolysis vapors using Pt and Mo-based catalysts

Supporting Information

Andreas Eschenbacher[a], Alireza Saraeian[b], Peter Arendt Jensen[a], Ulrik Birk Henriksen[a], Jesper Ahrenfeldt[a], Chengxin Li[c], Jens Øllgaard Duus[c], Asger Baltzer Hansen[e], Uffe Vie Mentzel[e], Brent H. Shanks[c], Anker Degn Jensen[a,]*

*corresponding author: aj@kt.dtu.dk

[a]*Department of Chemical and Biochemical Engineering, Technical University of Denmark (DTU), 2800 Kgs. Lyngby, Denmark*
[b]*Department of Chemical and Biological Engineering, Iowa State University, Ames, IA 50011, United States*
[c]*Department of Chemistry, Technical University of Denmark, 2800 Kgs. Lyngby, Denmark*
[e]*Haldor Topsøe A/S, 2800 Kgs. Lyngby, Denmark*

The supporting information consists of 18 pages, 5 tables and 26 figures.

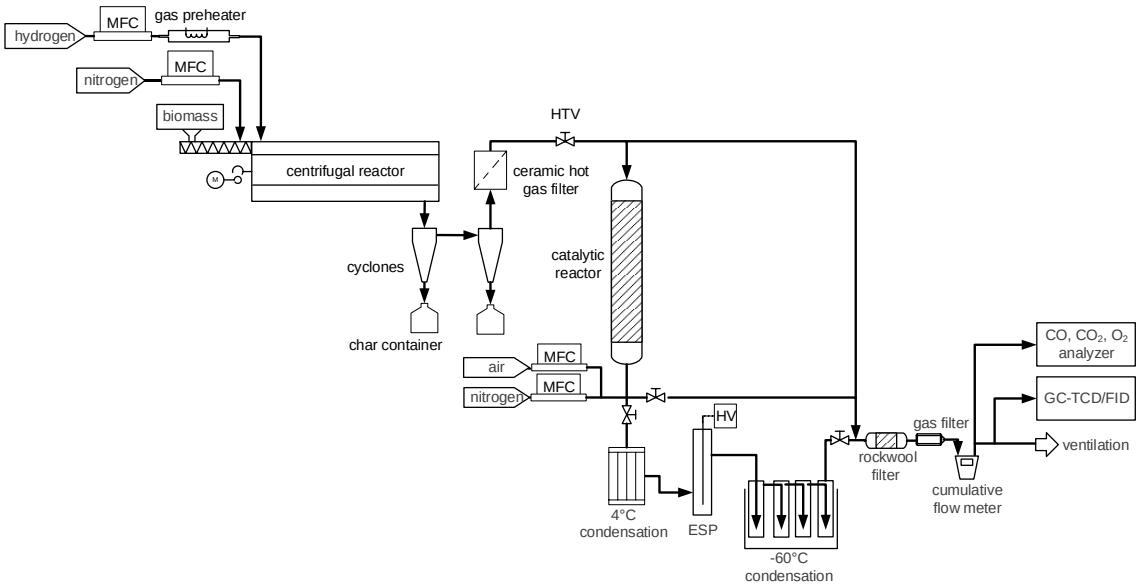

Fig. S1. Ablative fast pyrolysis unit with hot gas filtration and in-line catalytic upgrading of vapors prior to liquid condensation and gas analysis.

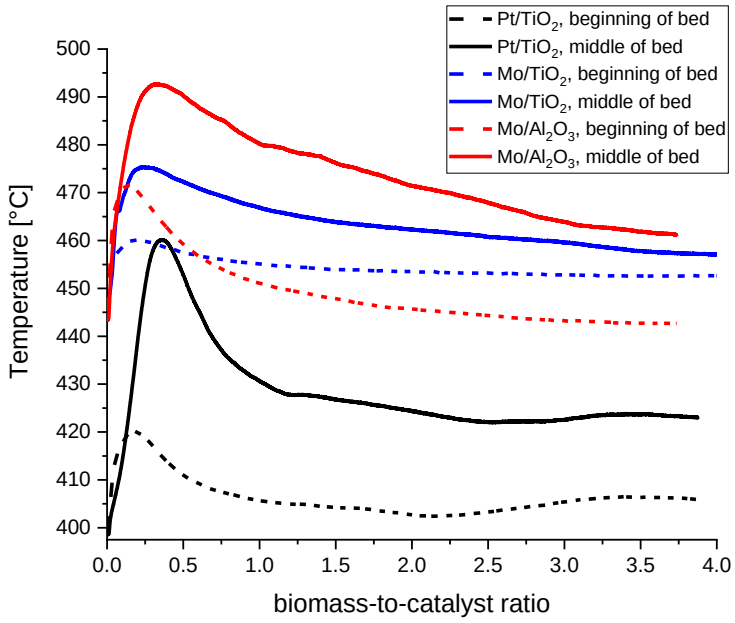

Fig. S2. Temperature of catalyst (100 g) during upgrading of wheat straw fast pyrolysis vapors with HDO catalysts at 50 vol.% H_2. The bed temperature was measured both at the beginning and the middle of the fixed bed.

Table S1. Yields (wt-% of daf biomass) for experiments conducted in 50 vol.% H_2.

Catalyst	-	Pt/TiO_2	Pt/TiO_2	Mo/Al_2O_3	Mo/Al_2O_3	MoO_3/TiO_2
B:C	-	1.4	3.9	3.7	7.2	4.1
C_1-C_3	0.9	2.9	3.4	2.6	2.4	1.9
$C_{2/3}$ olefins	0.4	0.8	0.9	1.5	1.3	1.0
CO	6.5	11.4	10.6	9.6	9.4	8.4
CO_2	11.1	18.5	14.8	16.4	15.0	14.2
Reaction water	18.7	23.2	23.1	25.2	26.0	24.2
organics in oil phase	8.4	1.7	2.4	2.6	1.8	4.0
organics in aqueous phase	25.0	14.5	17.0	12.7	15.4	18.3
C_4+ in gas	0.4	1.4	1.6	2.0	1.6	1.1
Coke	0.0	3.3	1.3	3.6	2.3	1.7
Char	18.3	18.1	18.8	19.2	19.8	19.7

Table S2. Yields (wt-% of daf biomass) for experiments conducted in 90 vol.% H_2.

Catalyst	Pt/TiO_2	Pt/TiO_2	MoO_3/TiO_2	MoO_3/TiO_2
B:C	3.9	8.2	3.6	7.3
C_1-C_3	3.7	3.4	2.4	2.2
$C_{2/3}$ olefins	0.8	0.8	1.3	1.1
CO	11.9	11.4	9.0	8.8
CO_2	19.7	15.6	16.9	14.7
Reaction water	20.9	20.9	26.2	24.5
organics in oil phase	1.9	2.4	2.2	3.7
organics in aqueous phase	19.4	20.6	18.2	18.6
C_4+ in gas	1.8	1.4	1.5	1.3
Coke	1.1	0.6	1.6	1.0
Char	15.8	18.9	19.2	20.8

Table S3. Yields (wt-% of daf biomass) for experiments conducted under N_2 atmosphere for empty reactor and 100 g TiO_2.

	empty (500 °C)	100 g TiO_2 (450 °C)
B:C	-	4.1
Yields (wt-% of daf biomass)		
H_2	0.0	0.2
C_1-C_3	0.8	1.3
$C_{2/3}$ olefins	0.4	0.6
CO	6.5	8.2
CO_2	11.3	15.1
Reaction water	17.3	20.8
organics in oil phase	24.6	19.9
organics in aqueous phase	11.3	4.2
C_4+ in gas	0.3	0.7
Coke	0.0	2.4

Table S4. Properties of bio-oil obtained in experiments conducted under N_2 atmosphere with empty reactor and 100 g TiO_2.

	empty (500 °C)	100 g TiO_2 (450 °C)
H_2O content [%]	11.0	6.3
wt-% N (d.b.)	3.0	2.3
wt-% C (d.b.)	63.1	69.9
wt-% H (d.b.)	7.2	7.5
wt-% O (d.b.)	26.7	20.3
Higher heating value (HHV) [MJ/kg]	27.7	31.1
Effective hydrogen index	0.6	0.8
H/C	1.4	1.3
O/C	0.3	0.2
TAN [mg KOH/g]	71.1	42.8

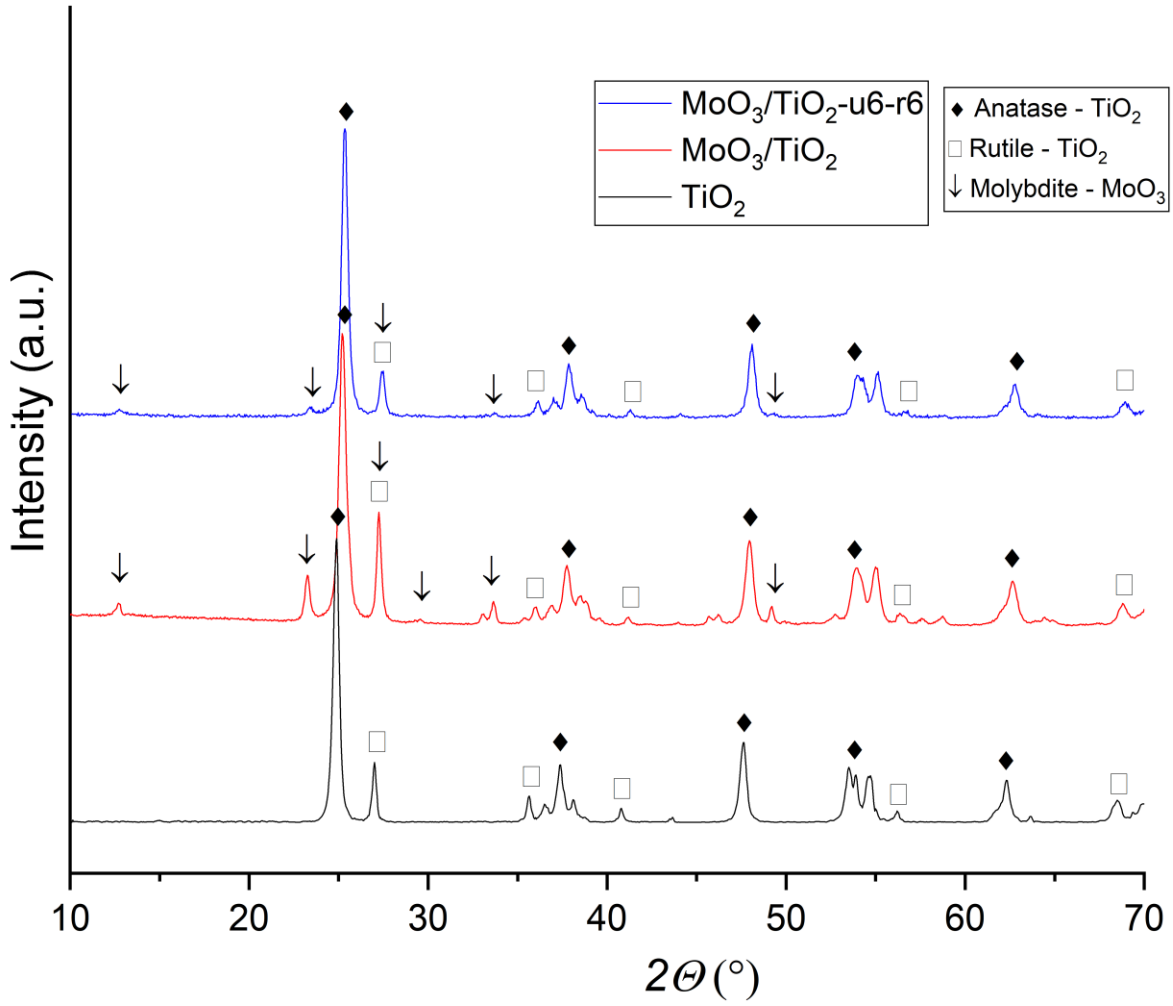

Fig. S3. Powder XRD patterns of the bare TiO_2 support and the fresh MoO_3/TiO_2 catalyst. Sample MoO_3/TiO_2-u6-r6 was used for six reaction-regeneration cycles. Wheat straw was used as feedstock for the first three cycles, after which lignin was used as feedstock for three additional cycles (not further detailed in this work).

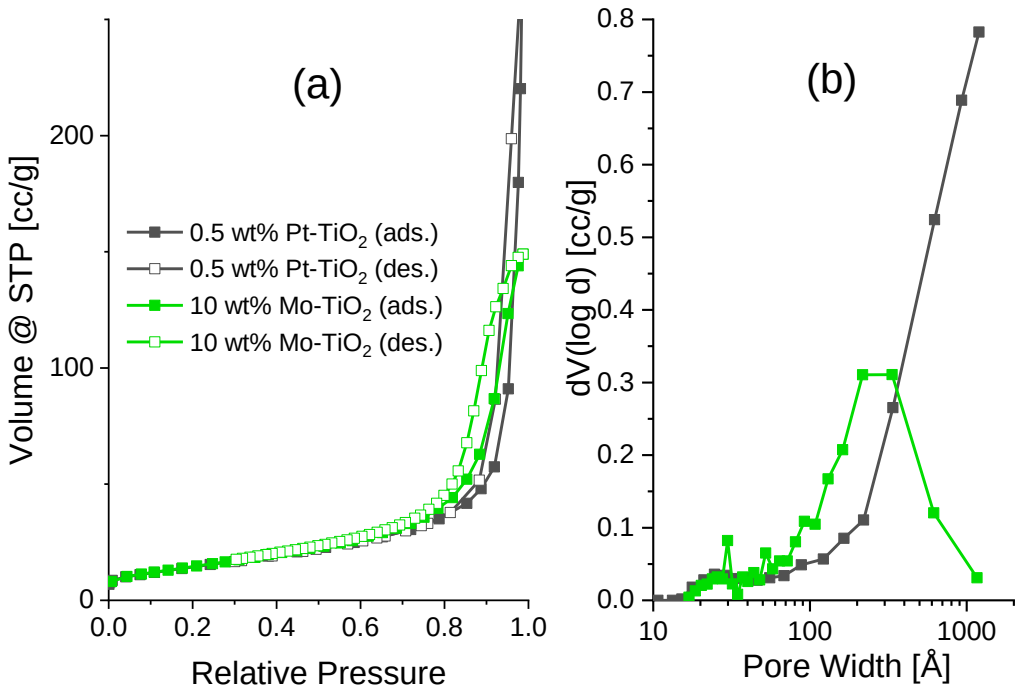

Fig. S4. (a) Isotherms from N_2 physisorption for TiO_2 supported Pt (0.5 wt%) and MoO_3 (10 wt%) catalysts. (b) BJH pore size distribution derived from adsorption isotherms shown in (a).

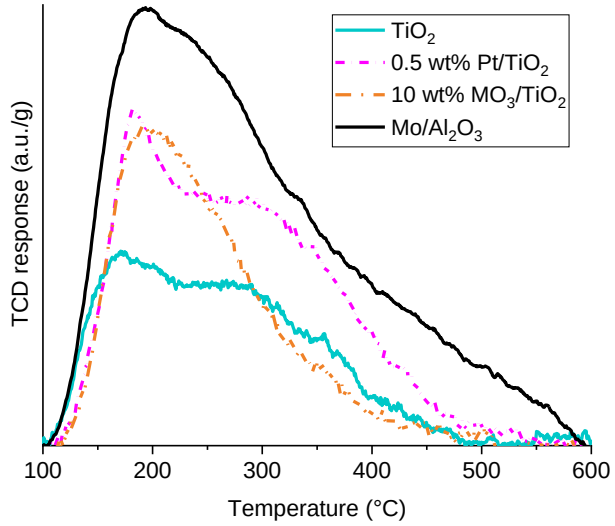

Fig. S5. NH_3-TPD of bare TiO_2, TiO_2 supported MoO_3 and Pt catalysts, and industrial Mo/Al_2O_3 catalyst. All catalysts were reduced prior to NH_3 adsorption.

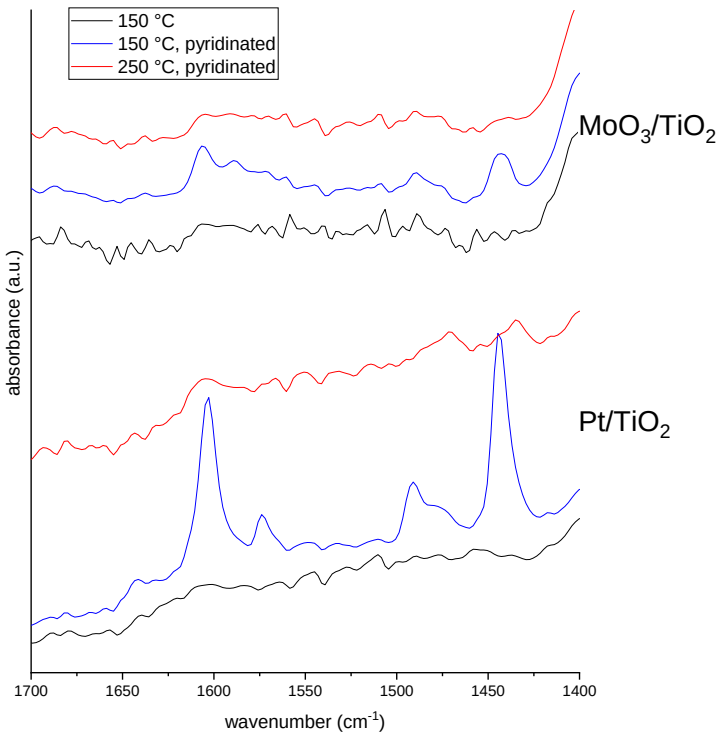

Fig. S6. 1700−1400 cm^{-1} region of Pyridine FT-IR for Pt/TiO_2 and MoO_3/TiO_2 catalyst. The samples were reduced for 1h at 450 °C prior to acquiring the non-pyridinated spectra (black) and adsorbing pyridine at 150 °C (blue).

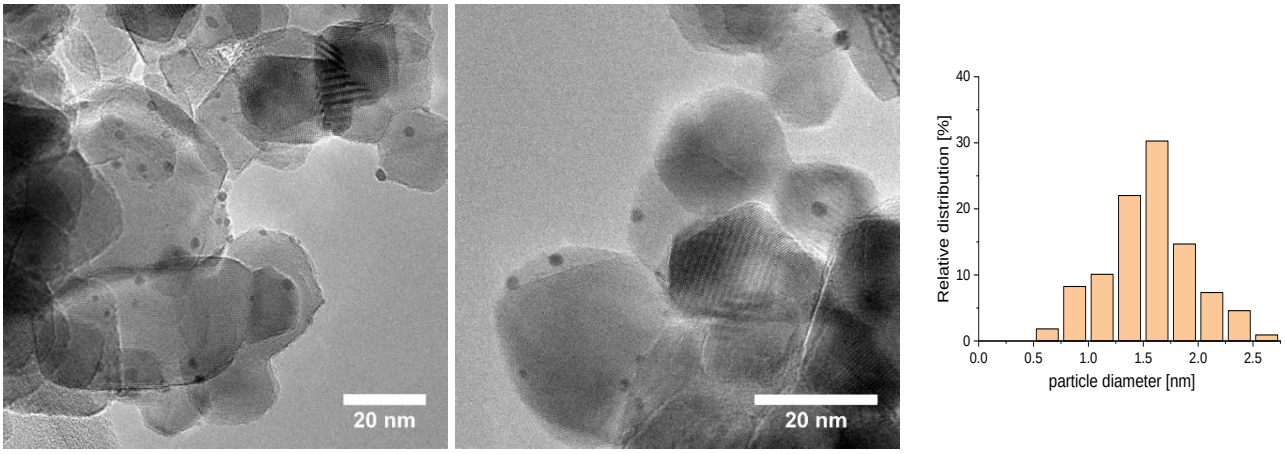

(a) (b) (c)

Fig. S7. Representative TEM images and particle size distributions on prepared Pt/TiO_2 catalyst (pre-reaction). The relative particle size distribution in **Fig. S7**c was derived from a count of 110 particles from ~10 different images acquired from different locations on the sample grid.

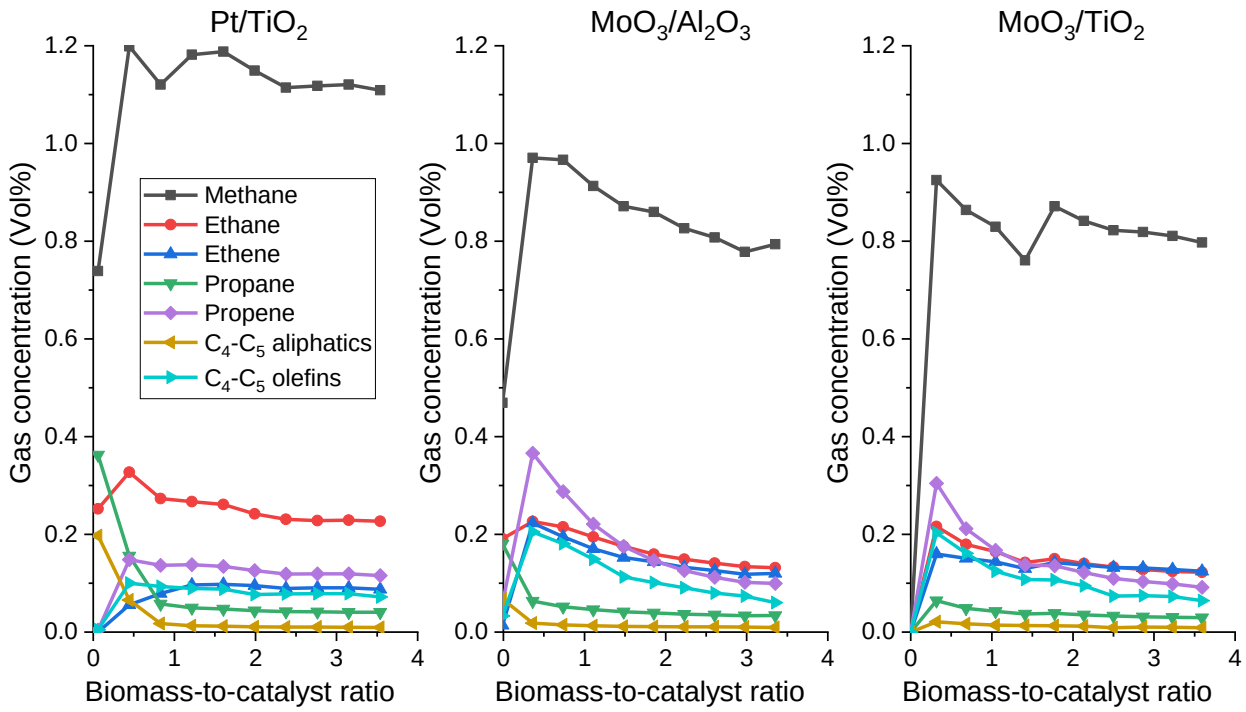

Fig. S8. Concentration of light hydrocarbons in the gas. Reaction atmosphere: 50 vol.% H_2. Catalyst temperature: 400 °C for Pt/TiO_2 and 450 °C for MoO_3-based catalysts.

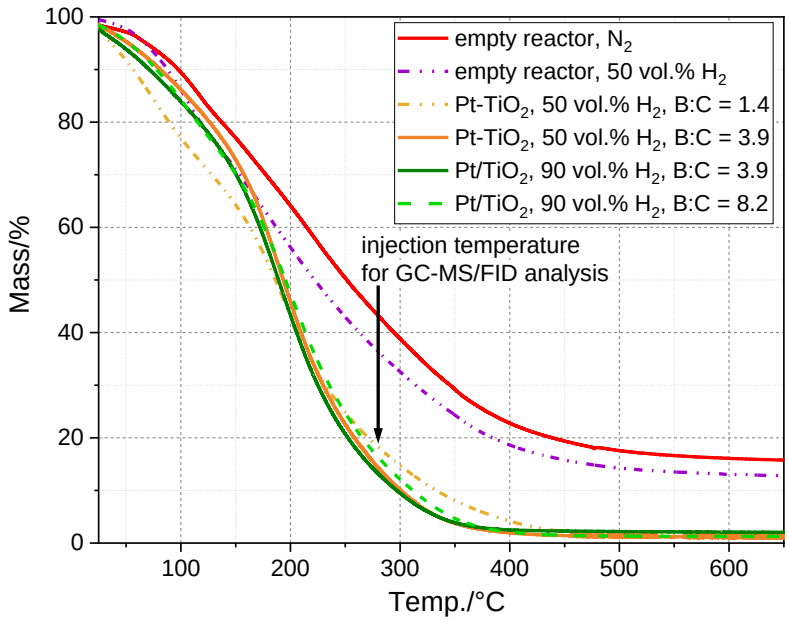

Fig. S9. TGA simulated distillation curves for the oils obtained with 100 g Pt-TiO_2 catalyst. About 20 mg of oil was prepared into a Pt crucible with lid shortly before start of the heating ramp in order to minimize the loss of volatiles.

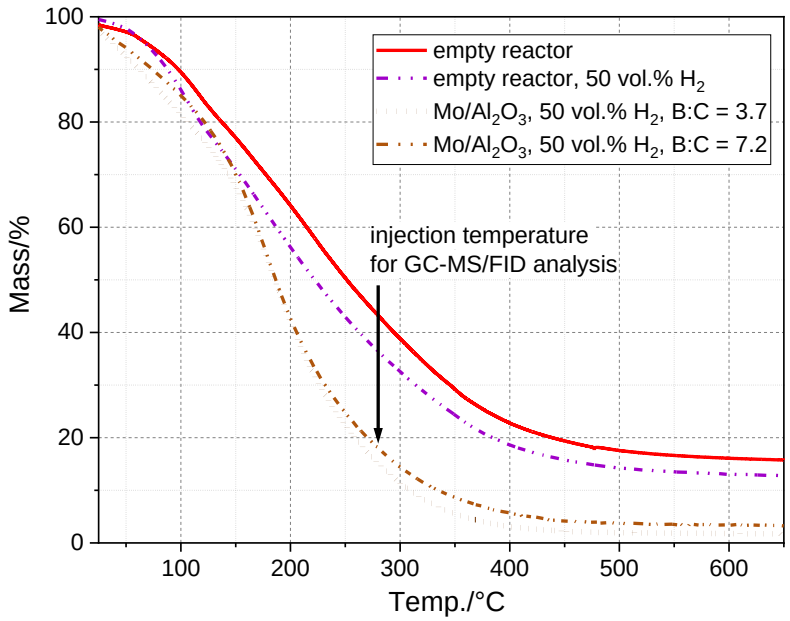

Fig. S10. TGA simulated distillation curves for the oils obtained with 100 g $MoO_3/Al2O3$ catalyst. About 20 mg of oil was prepared into a Pt crucible with lid shortly before start of the heating ramp in order to minimize the loss of volatiles.

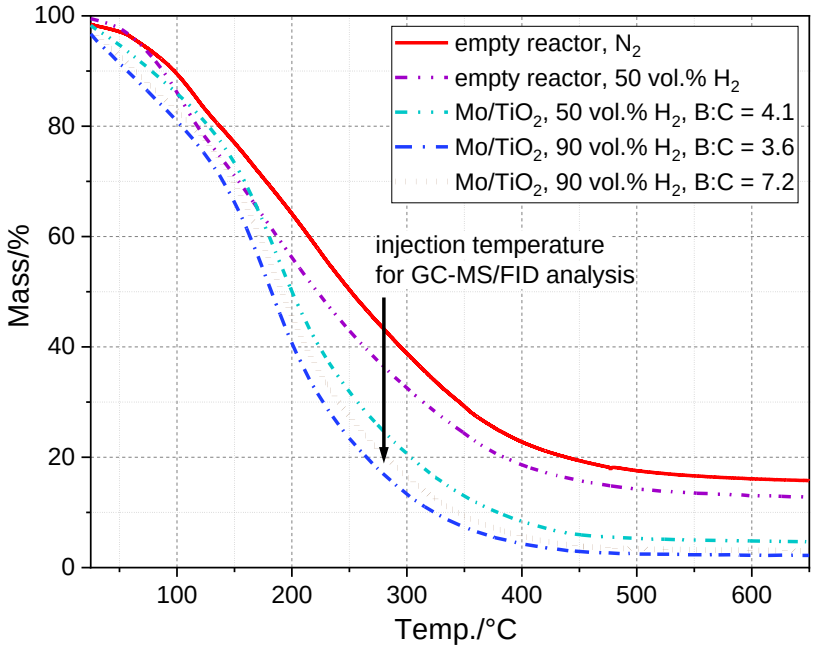

Fig. S11. TGA simulated distillation curves for the oils obtained with 100 g MoO_3/TiO_2 catalyst. About 20 mg of oil was prepared into a Pt crucible with lid shortly before start of the heating ramp in order to minimize the loss of volatiles.

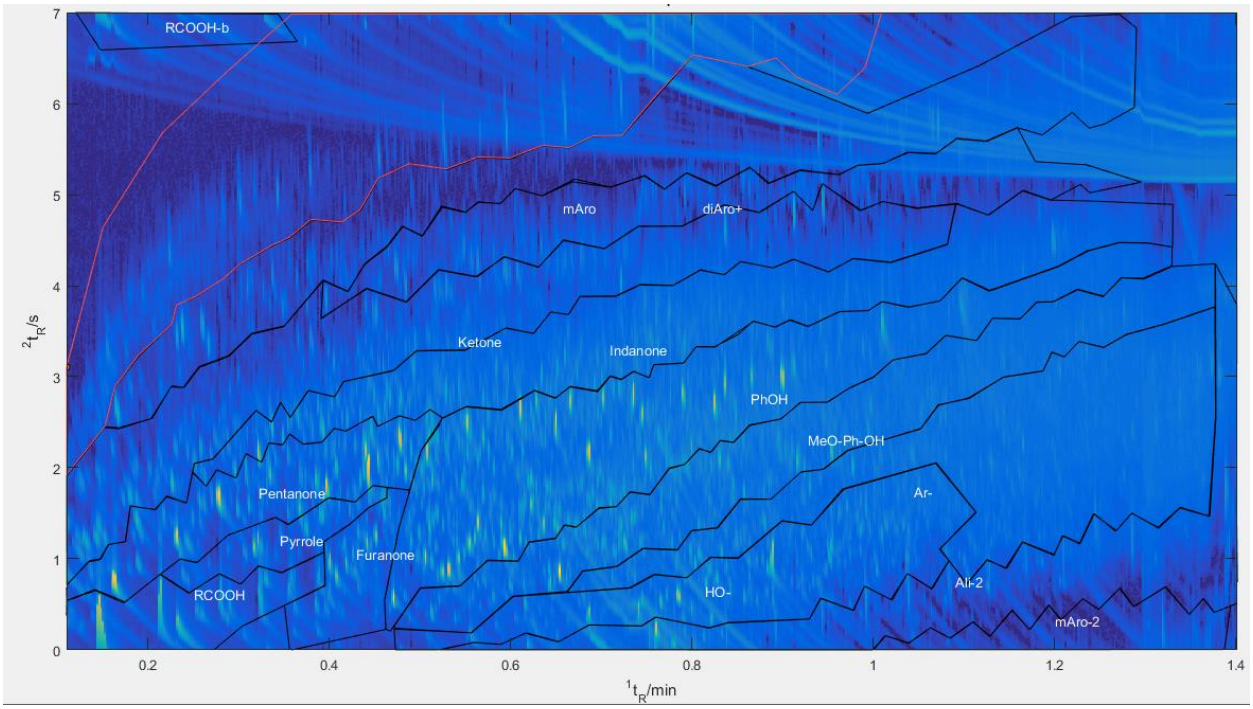

Fig. S12. 2D GC x GC plot of non-catalytic bio-oil collected at bench scale.

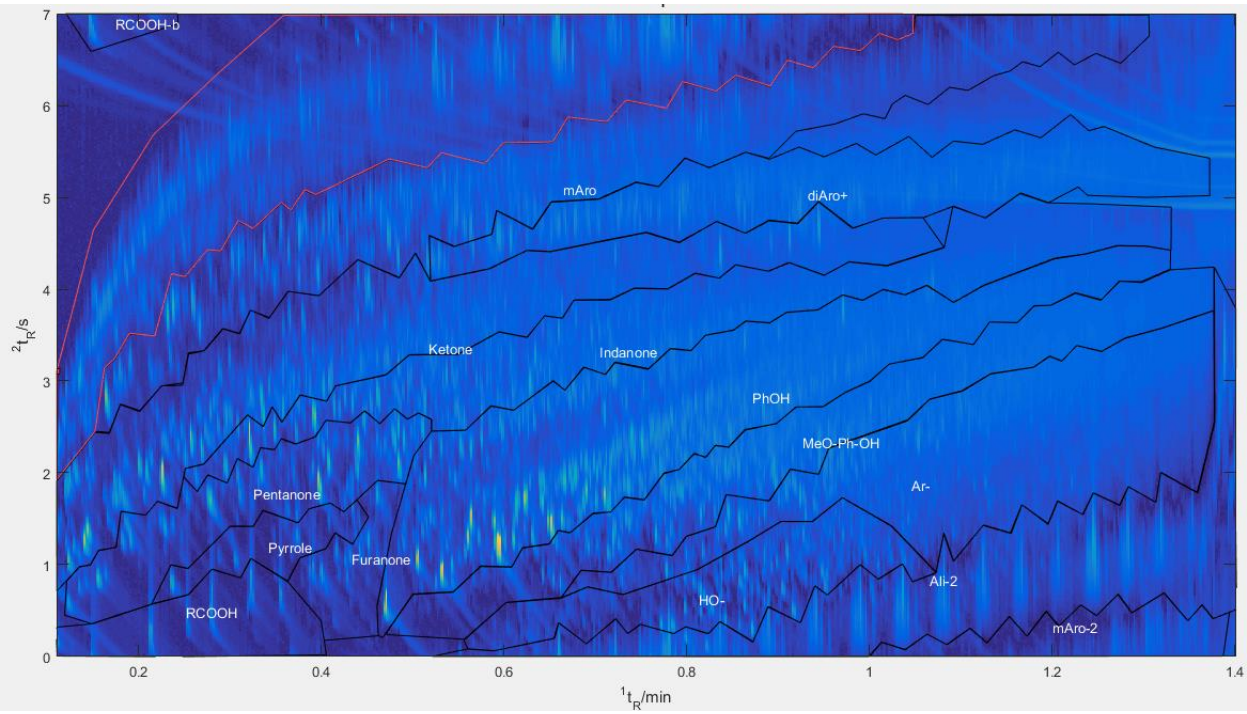

Fig. S13. 2D GC x GC plot of bio-oil obtained from vapor upgrading with Pt/TiO_2 catalyst at 400 °C, 50 vol.% H_2 and B:C ~4.

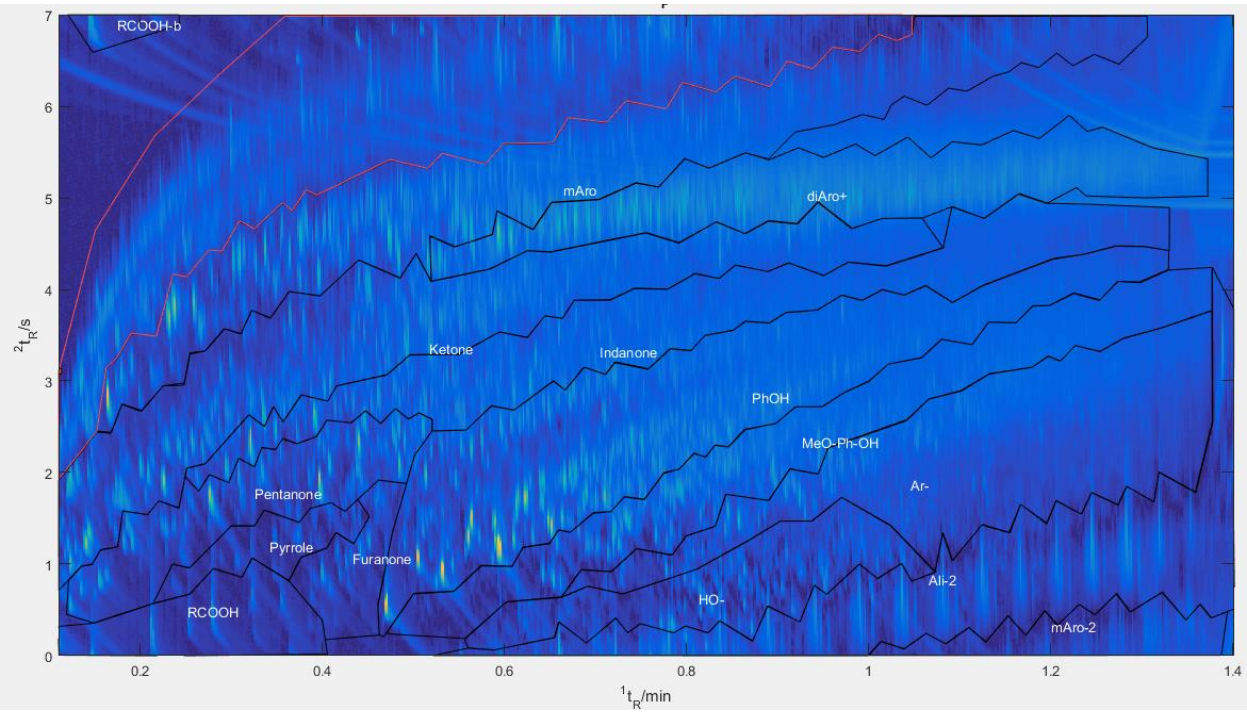

Fig. S14. 2D GC x GC plot of bio-oil obtained from vapor upgrading with MoO_3/Al_2O_3 catalyst at 450 °C, 50 vol.% H_2 and B:C ~4.

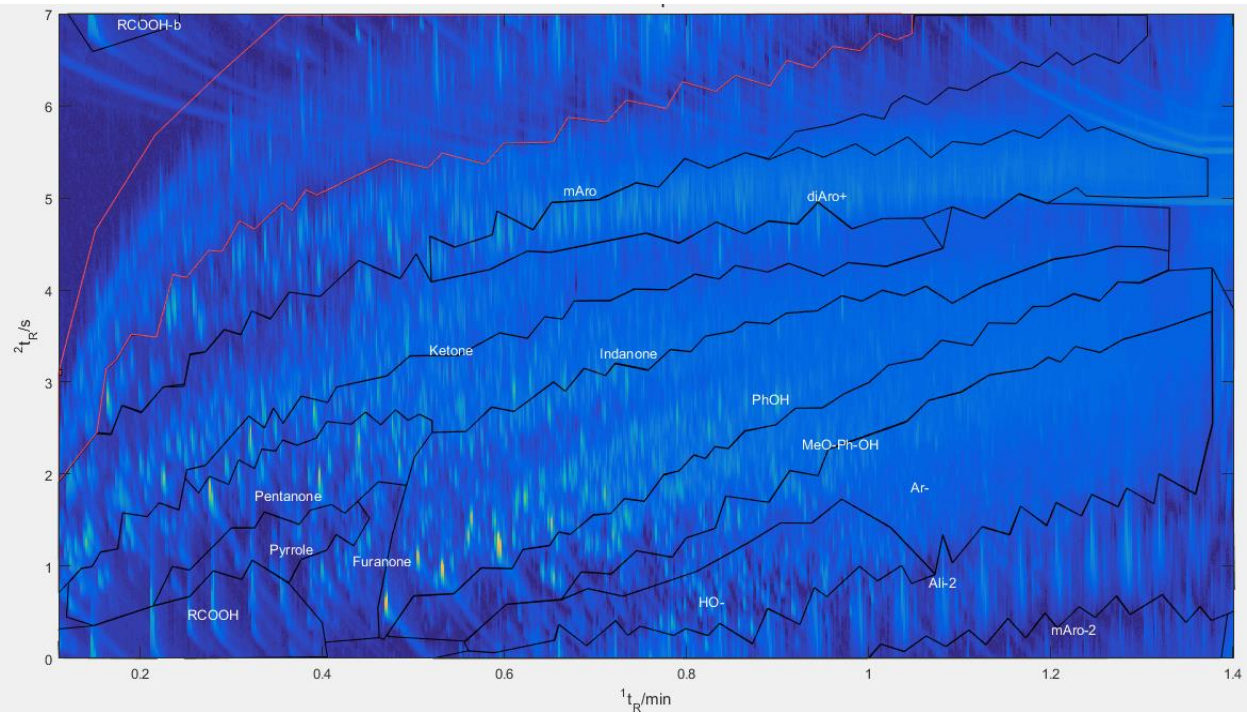

Fig. S15. 2D GC x GC plot of bio-oil obtained from vapor upgrading with MoO_3/TiO_2 catalyst at 450 °C, 50 vol.% H_2 and B:C ~4.

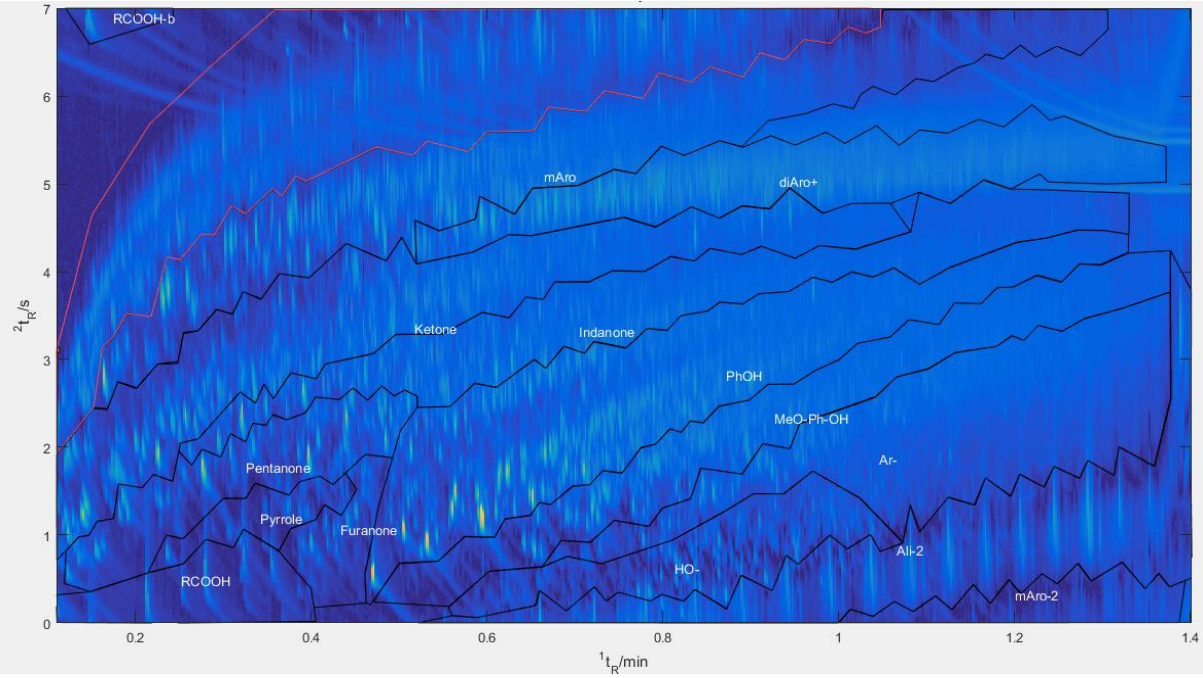

Fig. S16. 2D GC x GC plot of bio-oil obtained from vapor upgrading with MoO_3/TiO_2 catalyst at 450 °C, 90 vol.% H_2 and B:C ~4.

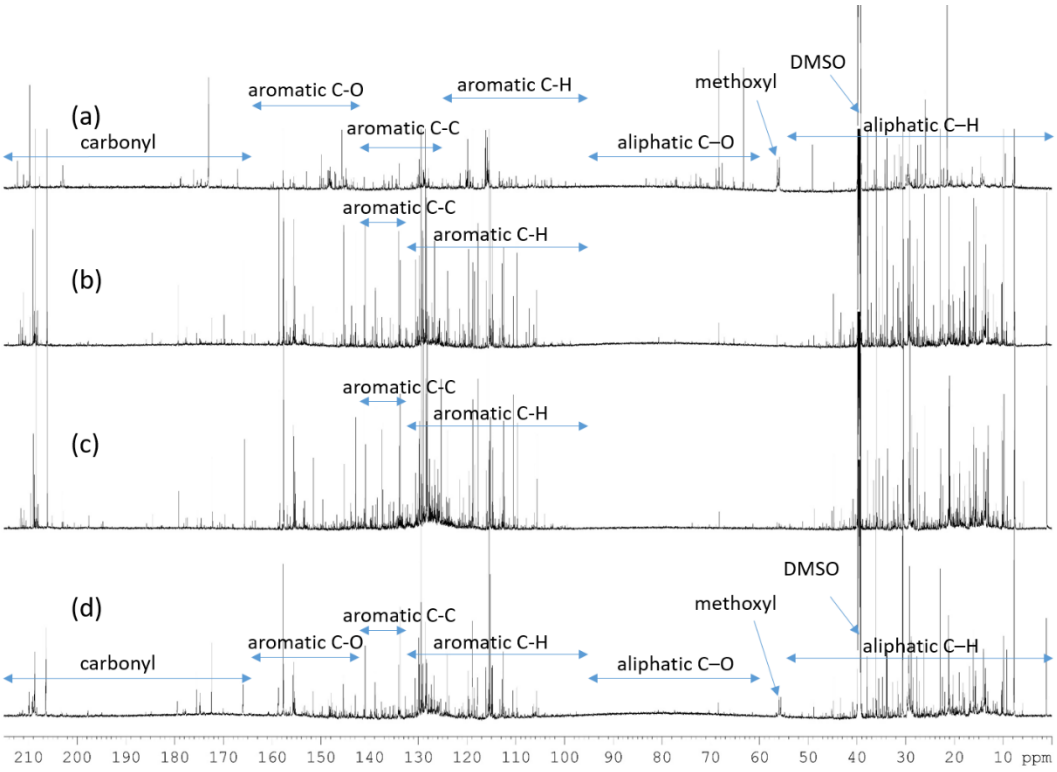

Fig. S17. ^{13}C NMR spectra of different bio-oils obtained at 50 vol.% H_2: (a) non-catalytic reference, (b) bio-oil obtained after in-line catalytic vapor treatment with 100 g Pt/TiO_2 catalyst at 400 °C and B:C ~4, (c) bio-oil obtained after in-line catalytic vapor treatment with 100 g MoO_3/Al_2O_3 catalyst at 450 °C and B:C ~4, and (d) bio-oil obtained after in-line catalytic vapor treatment with 100 g MoO_3/TiO_2 catalyst at 450 °C and B:C ~4.

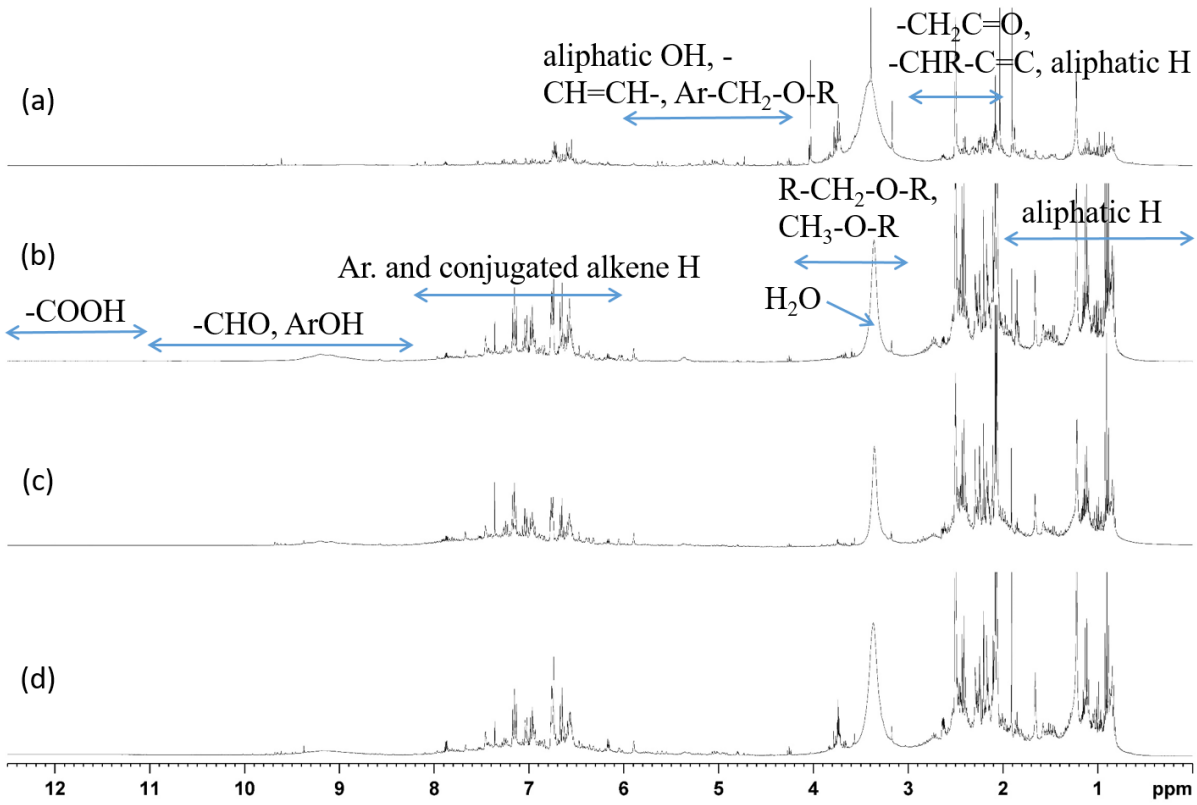

Fig. S18. ^{1}H NMR spectra of different bio-oils obtained at 50 vol.% H_2: (a) non-catalytic reference, (b) bio-oil obtained after in-line catalytic vapor treatment with 100 g Pt/TiO_2 catalyst at 400 °C and B:C ~4, (c) bio-oil obtained after in-line catalytic vapor treatment with 100 g MoO_3/Al_2O_3 catalyst at 450 °C and B:C ~4, and (d) bio-oil obtained after in-line catalytic vapor treatment with 100 g MoO_3/TiO_2 catalyst at 450 °C and B:C ~4.

Table S5. Carbon percentage based on the ^{13}C NMR analysis of non-catalytic bio-oil and bio-oil obtained from vapor upgrading with MoO_3/TiO_2.

	No catalyst	MoO_3/TiO_2	MoO_3/TiO_2
H_2 vol.%, B:C	50 vol.%	50 vol.%, B:C = 4.1	90 vol.%, B:C = 7.3
Carbonyl (215–166.5 ppm)	15.4%	9.3%	10.1%
Aromatic C–O (166.5–142 ppm)	12.5%	10.3%	9.8%
Aromatic C–C (142–132/125 ppm)[a]	9.2%	5.4%	4.7%
Aromatic C–H (132/125–95.8 ppm)[a]	16.5%	26.4%	27.5%
Aliphatic C–O (95.8–60.8 ppm)	9.9%	2.4%	2.7%
Methoxyl (60.8–55.2)	4.2%	1.3%	1.3%
Aliphatic C–H (55.2–0 ppm, with exclusion of solvent)	32.4%	44.8%	43.8%

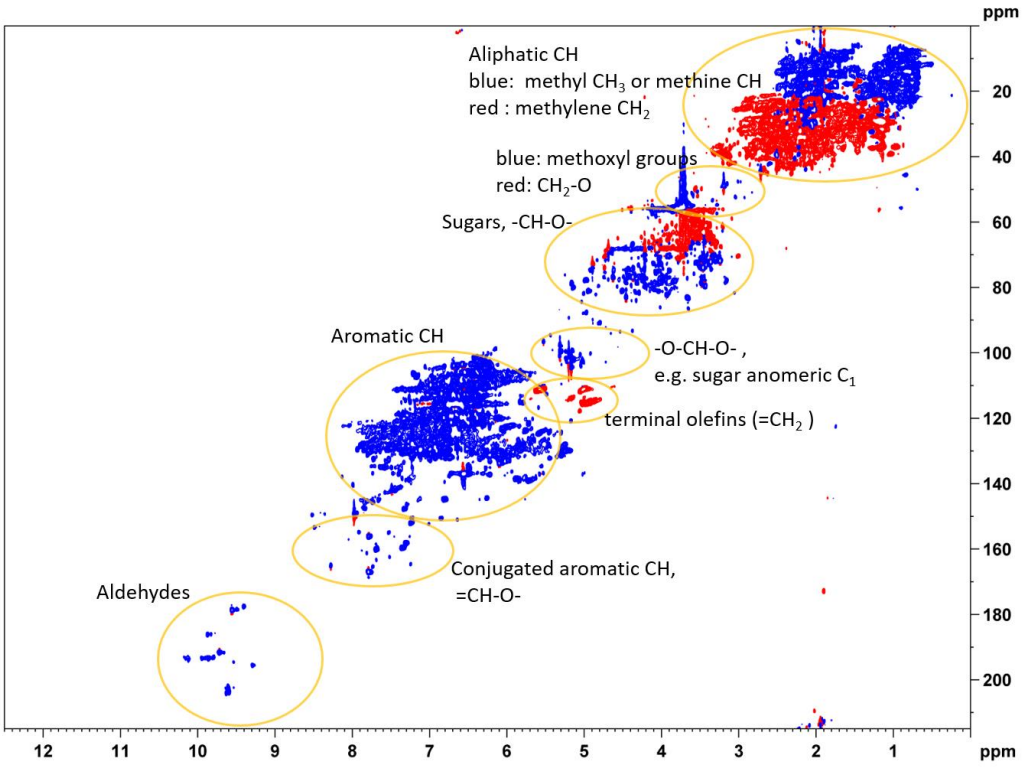

Fig. S19. 2D NMR spectra of bio-oil obtained with empty catalytic reactor at 50 vol.% H_2.

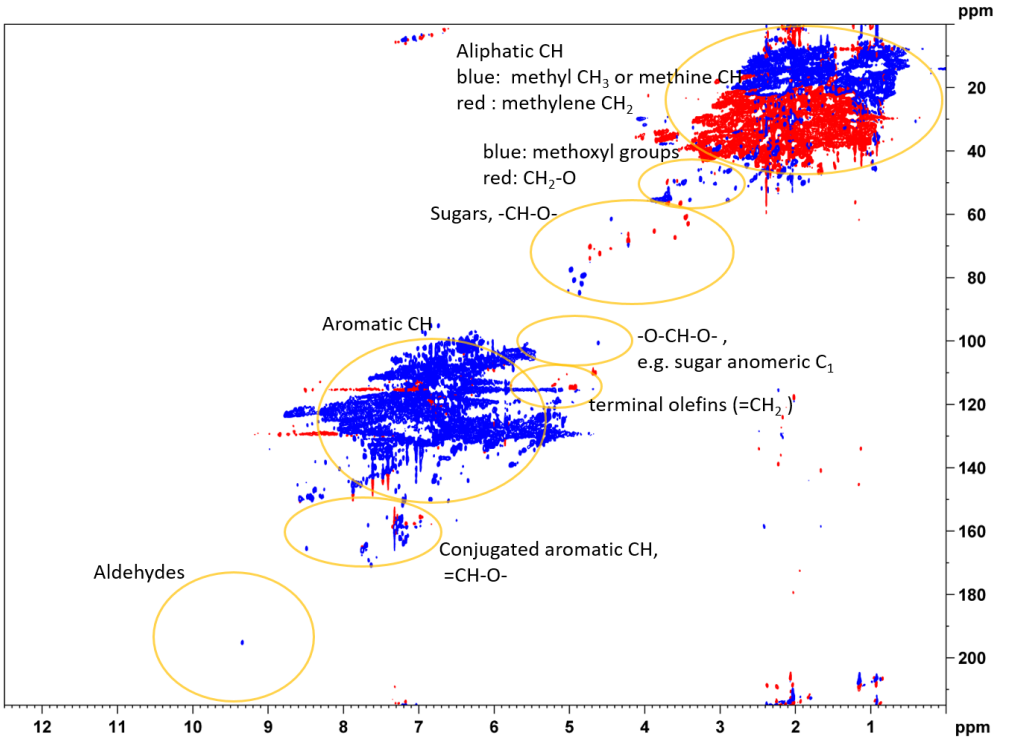

Fig. S20. 2D NMR spectra of bio-oil obtained with 100 g Pt/TiO_2 catalyst at 400 °C and 50 vol.% H_2, operated to B:C ~4.

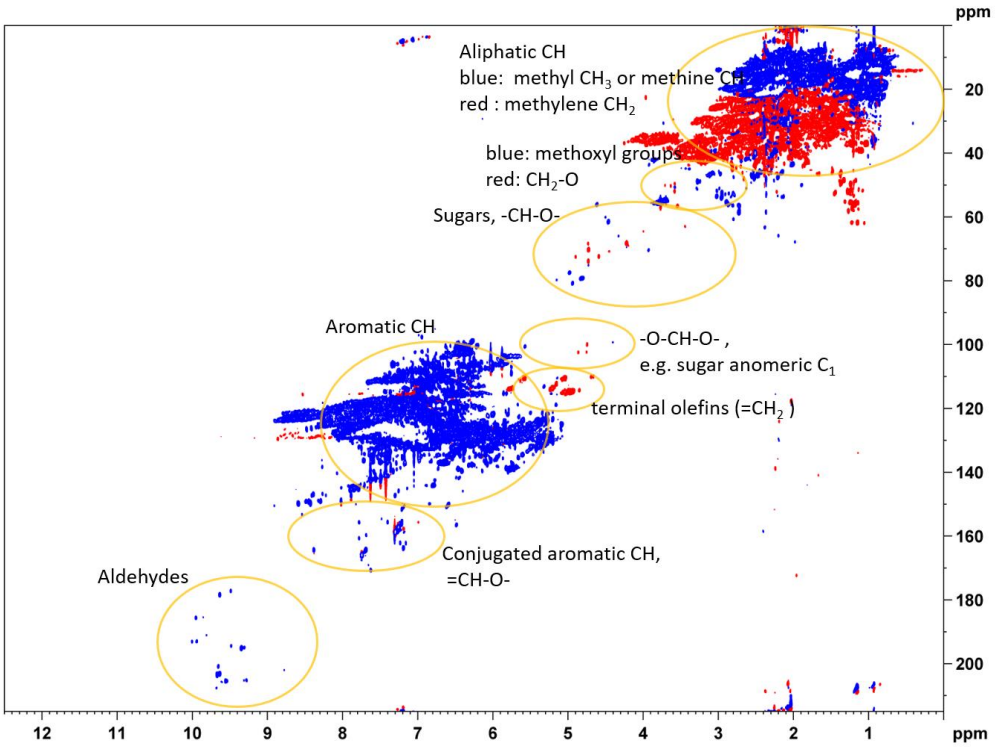

Fig. S21. 2D NMR spectra of bio-oil obtained with 100 g of an industrial MoO3/Al2O3 catalyst at 450 °C and 50 vol.% H2, operated to B:C ~4.

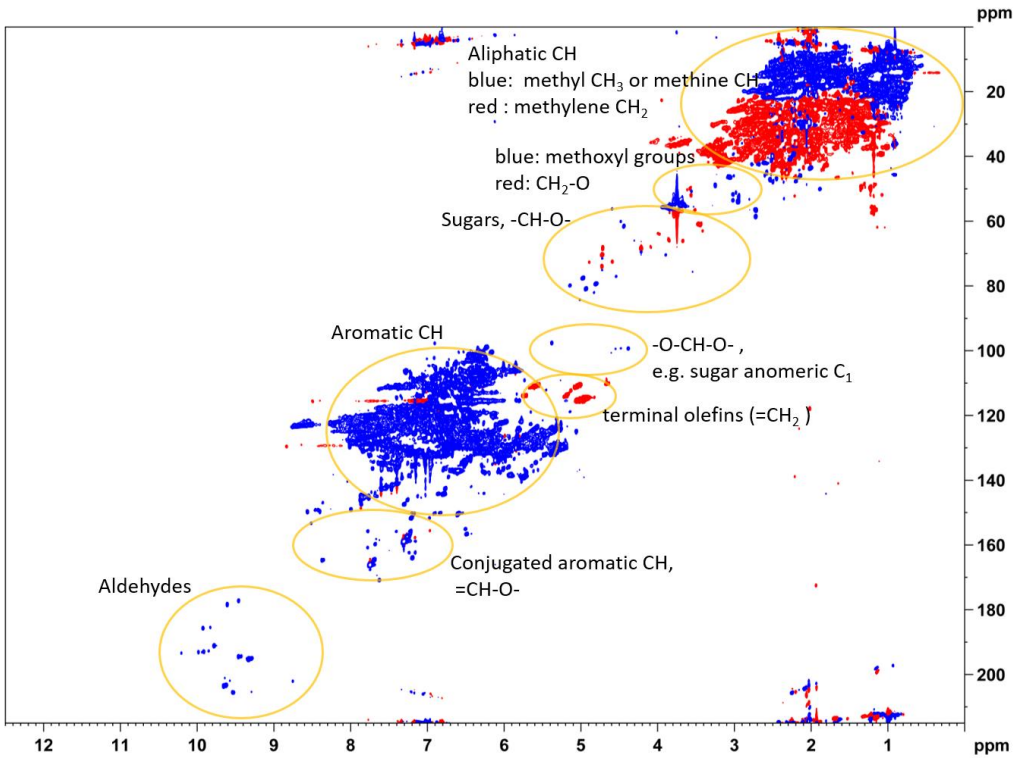

Fig. S22. 2D NMR spectra of bio-oil obtained with 100 g MoO_3/TiO_2 catalyst at 450 °C and 50 vol.% H_2, operated to B:C ~4.

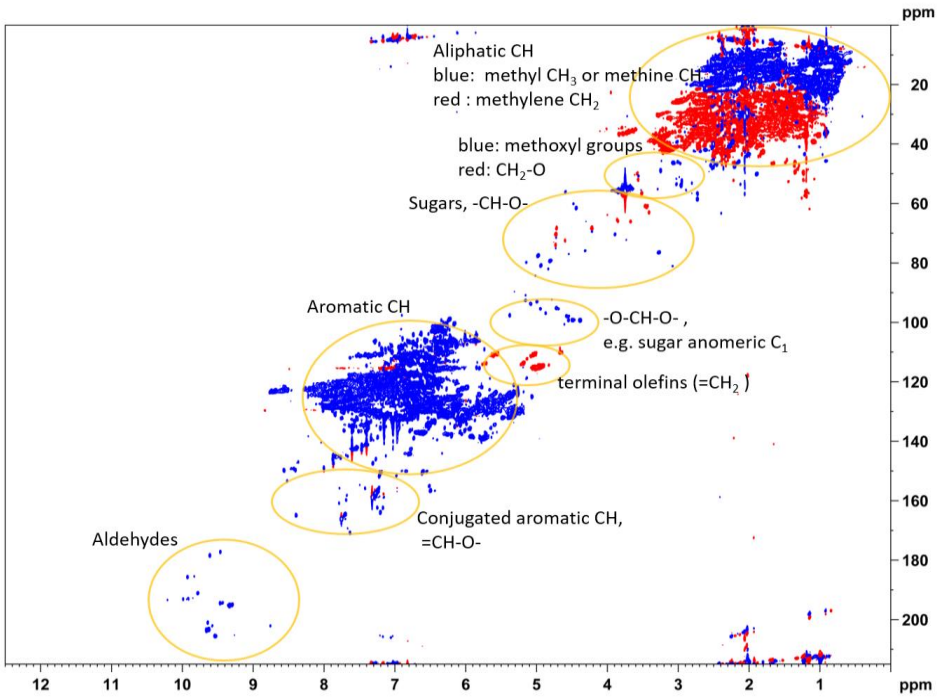

Fig. S23. 2D NMR spectra of bio-oil obtained with 100 g MoO_3/TiO_2 catalyst at 450 °C and 90 vol.% H_2, operated to B:C ~7.

Equilibrium calculations

Equilibrium concentrations were calculated using the HSC Chemistry 9 software package. The calculations were performed with equal fractions of each molecule and 99% H_2. The sum of the species in each category (aromatics/napthenes) is shown.

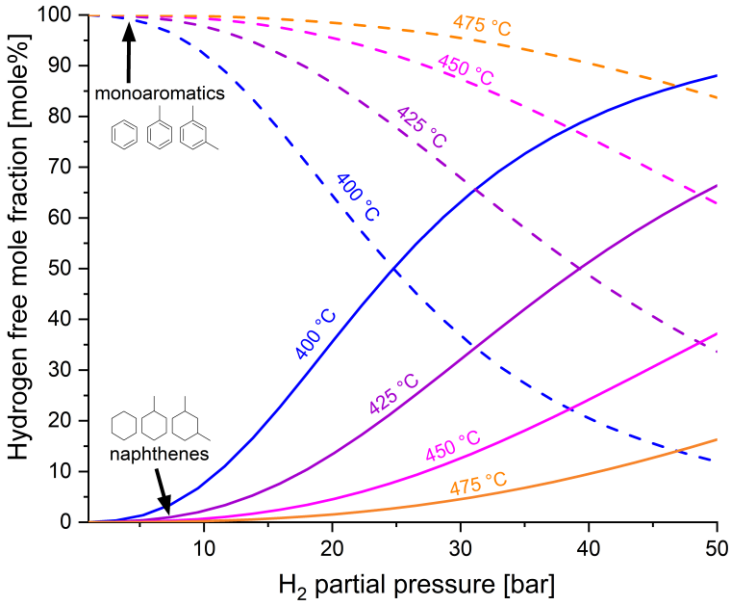

Fig. S24. The influence of the total pressure and different temperatures on the equilibrium distribution between monoaromatics and their hydrogenated versions.

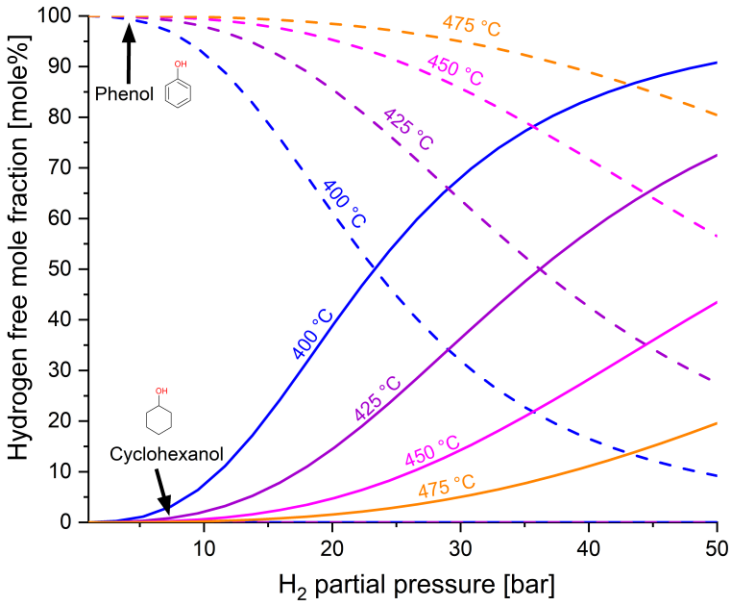

Fig. S25. The influence of the total pressure and different temperatures on the equilibrium distribution between phenol and cyclohexanol.

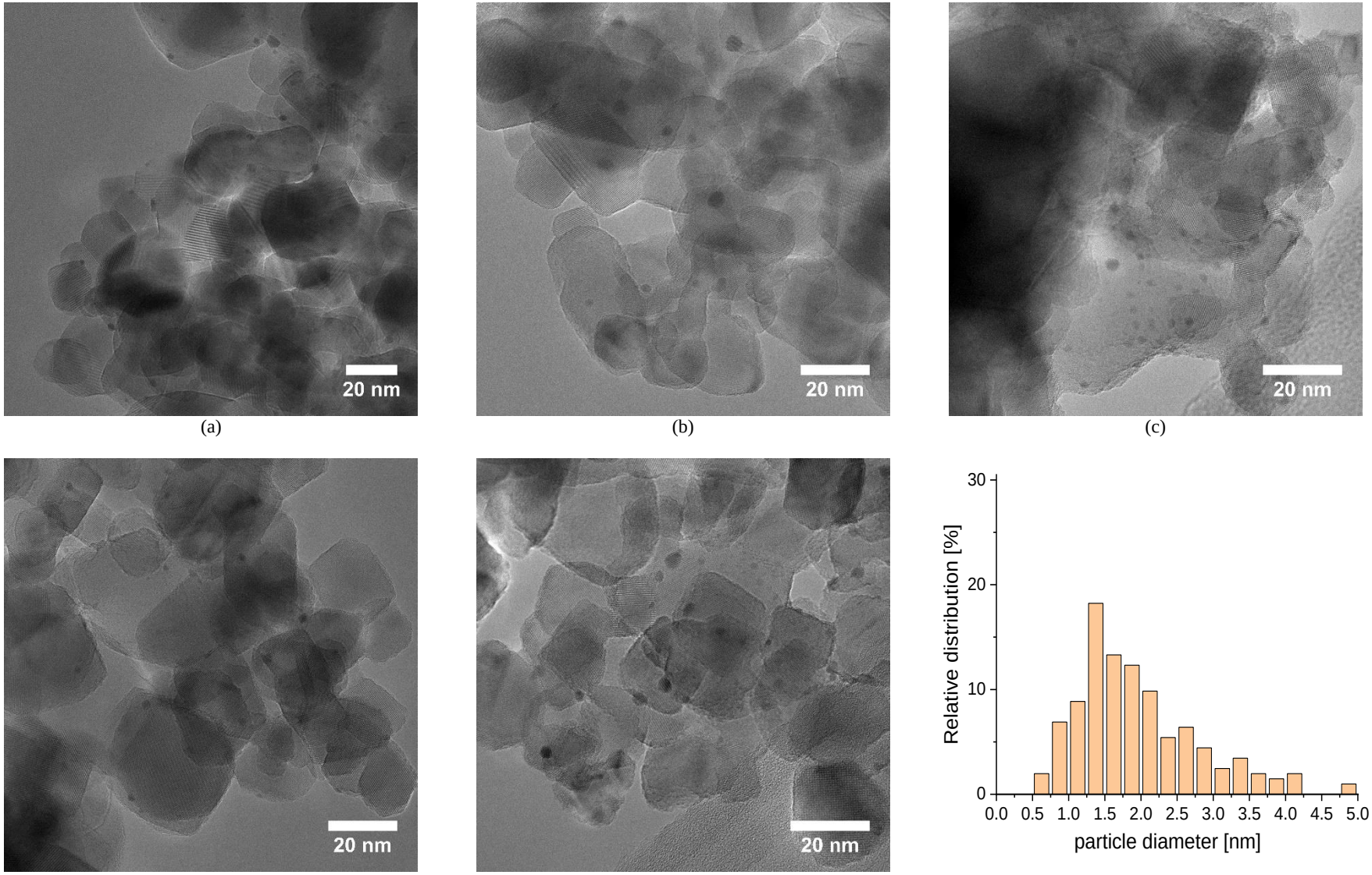

(a) (b) (c)

(d) (e) (f)

Fig. S26. (a)-(e) Representative TEM images of the post-reaction TiO_2 supported Pt (0.6 wt%) catalyst, i.e. after four reaction/regeneration cycles. (f) Particle size distributions was derived from a count of ~200 particles from 10 different locations/images.